CHEMISTRY
AN ASIAN JOURNAL

DOI: 10.1002/asia.200900627

Complex Kinetics of Fluctuating Enzymes: Phase Diagram Characterization of a Minimal Kinetic Scheme

Wei Min,[a] Liang Jiang,[b] and X. Sunney Xie*[a]

Dedicated to the 100th anniversary of the College of Chemistry, Peking University

Abstract: Enzyme molecules are dynamic entities with stochastic fluctuation in both protein conformation and enzymatic activity. However, such a notion of fluctuating enzymes, best characterized by recent single-molecule experiments, was not considered in the classic Michaelis–Menten (MM) kinetic scheme. Here we incorporate the fluctuation concept into the reversible MM scheme, and solve analytically all the possible kinetics (i.e., substrate concentration dependent enzymatic velocity) for a minimal model of fluctuating enzymes. Such a minimal model is found to display a variety of distinct kinetic behaviors (phases) in addition to the classic MM kinetics; excess substrate inhibition, sigmoidal kinetics, and concave biphasic kinetics. We find that all these kinetic phases are interrelated and unified under the framework of fluctuating enzymes and can be adequately described by a phase diagram that consists of two master parameters. Functionally, substrate inhibition, sigmoidal kinetics, and convex biphasic phases exhibit positive cooperativity, whereas concave biphasic phases display negative cooperativity. Remarkably, all these complex kinetics are produced by fluctuating enzymes with single substrate binding site, but the two conformations are, therefore, fundamentally different from the classic MWC and KNF models that require multiple subunit or binding sites. This model also suggests that, for a given enzyme/substrate pair, the non-MM behaviors could undergo transitions among different kinetic phases induced by varying product concentrations, owing to the fundamental Haldane symmetry in the reversible MM scheme.

Keywords: cooperative effects · enzymes · kinetics · phase diagrams

Introduction

Enzymes are central to biochemical processes occurring in live cells, and are extraordinary biological catalysts. An enzyme can accelerate the rate of biochemical reactions by many orders of magnitude,[1] but is left unchanged at the end of the reaction, and, therefore, leaves the equilibria unaltered. It binds a specific reactant, called a substrate, and facilitates its reaction by stabilizing its transition state, leading to its product. A powerful strategy to studying the mechanism of an enzyme-catalyzed reaction is to determine the rate of the reaction and how it changes in response to changes in experimental parameters.[2] Such a kinetic study is the traditional approach to understanding enzyme mechanisms and remains one of the most important.[3–6]

Enzyme kinetics is usually described by the reversible Michaelis–Menten (MM) scheme (Scheme 1).[7–9] The resulting MM equation shows hyperbolic dependence on substrate and product concentrations. The kinetics and thermodynamics revealed by this simple scheme are straightforward and well understood.

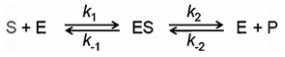

Scheme 1. Classic reversible Michaelis–Menten kinetics.

[a] Dr. W. Min,[+] Prof. X. S. Xie
Department of Chemistry and Chemical Biology
Harvard University, Cambridge, MA 02138 (USA)
Fax: 617-496-8709
E-mail: xie@chemistry.harvard.edu

[b] Dr. L. Jiang[++]
Department of Physics
Harvard University
Cambridge, MA 02138 (USA)

[++] Current address: Institute for Quantum Information
California Institute of Technology
Pasadena, CA 91125 (USA)

[+] These two authors have contributed equally to this work.

However, recent single-molecule enzymatic assays have revealed a surprisingly dynamic property of enzyme molecules, which is usually hidden in the conventional ensemble measurements—during catalysis, enzyme molecules fluctuate at both the conformation[10–15] and chemical-activity levels[16–24] over broadly distributed enzymatically relevant time scales ranging from 10^{-5} to 100 seconds. These dynamic fluctuations in conformation and catalytic activity could either arise from thermal fluctuations[12–15] or substrate-induced conformational motions.[25] The broad range of enzyme systems that these observations have been made on suggests the generality of the concept of fluctuating enzymes. Apparently, this concept was not explicitly included in the classic MM scheme, which serves as the theoretical motivation of the present study.

The strong motivation on the enzymology side comes from accumulated experimental observations on many monomeric enzyme systems (summarized in Refs. [50–64]). These systems have been measured to display distinct non-MM kinetics, such as positive and negative cooperativity and substrate inhibition. They are all *monomeric* in function, which excludes the interpretation of classic Monod–Wyman–Changeux (MWC) and Koshland–Nemethy–Filmer (KNF) models that require multiple subunits or binding sites. The exact responsible mechanisms are not clear yet and still under debate in the literature. It was hypothesized that the fluctuating enzyme notion we investigate in this paper could contribute to the observed but unexplained non-MM kinetics of monomeric enzymes.

The goal of this paper is to first develop a minimal scheme for fluctuating enzymes and then analytically dissect all the possible kinetic behaviors. We begin with descriptions of the classic reversible MM kinetics, and then investigate the enzyme kinetics of the minimal kinetic scheme. Detailed complex kinetic behaviors, a unified description of a two-dimensional phase diagram, and the product induced phase transitions are then provided analytically, accompanied by concrete numerical examples. We end with a brief summary on the implications and lessons learnt from this minimal model of fluctuating enzymes.

Results and Discussions

Classic Reversible Michaelis–Menten Kinetics

In Scheme 1, the catalysis step is generally reversible when the enzyme is present in the cellular soup where significant amounts of both substrates and products exist in vivo, but it is often treated as irreversible when the mechanism applies strictly to the initial rate of the reaction in vitro before the product concentration has become appreciable. In the presence of both $[S]$ and $[P]$, the net enzyme velocity v_{net} of the classic reversible MM scheme has the following form [Eq. (1)]:[5,6]

$$v_{net} = \frac{k_1 k_2 [S] - k_{-1} k_{-2} [P]}{k_{-1} + k_2 + k_1 [S] + k_{-2} [P]} \tag{1}$$

When and only when $[S]$ and $[P]$ are in their chemical equilibrium, v_{net} is zero, and we have the well-known Haldane relationship [Eq. (2)]:[9]

$$\frac{k_1 k_2}{k_{-1} k_{-2}} = \left(\frac{[P]}{[S]}\right)_{eq} = K_{eq} \tag{2}$$

in which K_{eq} is the equilibrium constant. The Haldane relationship means that the enzyme accelerates both the forward and backward reactions, thus would not alter the chemical equilibrium between substrate and product. If $[S]$ and $[P]$ are not in equilibrium in general, we define [Eq. (3)]:

$$\Delta S \equiv [S] - [S]_{eq} = [S] - \frac{[P]}{K_{eq}} \tag{3}$$

then Equation (1) can be written as Equation (4):

$$v_{net} = \frac{k_2 \Delta S}{\left(\frac{k_{-1} + k_2 + k_{-2}[P]}{k_1} + \frac{[P]}{K_{eq}}\right) + \Delta S} \tag{4}$$

For quantitative purposes it is more useful to linearize Equation (4). In this paper, we prefer to utilize the Eadie–Hofstee (EH) plot. It is well know that the EH plot is more sensitive to the deviation from MM kinetics, particularly because the EH plot gives equal weight to data points in any range of substrate concentration or reaction velocity.[6] In contrast, the Lineweaver–Burke plot unevenly weighs such points. For the normal EH plot, $[P]$ is zero, and v is plotted directly as a function of $v/[S]$. Here we deal with v_{net} and non-zero $[P]$, therefore we employ a generalized EH plot where v_{net} is plotted as a function of $v_{net}/\Delta S$. Equation (4) rearranges to a straight line [Eq. (5)]:

$$v_{net} = k_2 - K_M^{[P]} (v_{net}/\Delta S) \tag{5}$$

The negative slope of which is the new apparent Michaelis constant $K_M^{[P]}$, which is a first order equation on $[P]$, [Eq. (6)]:

$$K_M^{[P]} = \frac{k_{-1} + k_2 + k_{-2}[P]}{k_1} + \frac{[P]}{K_{eq}} \tag{6}$$

Therefore, for the classic reversible MM scheme, the only effect of product concentration is to increase the apparent Michaelis constant $K_M^{[P]}$, modifying the negative slope of the straight line in the generalized EH plot. In essence, such an inhibition effect of product concentration on the overall kinetics is similar to that of a competitive inhibitor that only affects the apparent Michaelis constant but not the turnover rate k_2.[5,6]

CHEMISTRY
AN ASIAN JOURNAL

Minimal Kinetic Scheme of Fluctuating Enzymes

Motivated by recent single-molecule experimental observations of enzyme conformation and catalytic activity fluctuations[10–24] over broadly distributed time scales, we introduce Scheme 2, which is the minimal kinetic scheme of fluctuating enzymes. In contrast to the classic reversible MM Scheme 1, in which both the free enzyme E and enzyme-substrate complex ES are well-defined non-fluctuating states, Scheme 2 has two E states and two ES states with different catalytic activities, interconnected through protein conformational dynamics. Note that the conformational dynamics occurring between ES_1 and ES_2, whose rate constants are denoted as β_{12} and β_{21}, could either be spontaneous thermal motion[12–15] or be functionally important induced by substrate (or product) binding.[25]

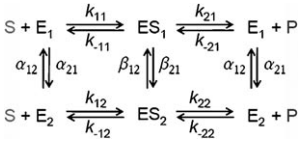

Scheme 2. Reversible Michaelis–Menten kinetics of fluctuating enzymes.

In Scheme 2, the rate constants cannot be arbitrary. First, the Haldane relation Equation (2) applies for both channels [Eq. (7)]:

$$\frac{k_{11}k_{21}}{k_{-11}k_{-21}} = \frac{k_{12}k_{22}}{k_{-12}k_{-22}} = K_{eq} \tag{7}$$

Second, both the substrate binding/dissociation loop (the left loop in Scheme 2) and product binding/dissociation loop (the right loop in Scheme 2) follow the fundamental detailed balance condition which is the consequence of microscopic reversibility of the underlying mechanics [Eq. (8)]:[26,27]

$$\frac{k_{11}\beta_{21}k_{-12}\alpha_{12}}{k_{-11}\beta_{12}k_{12}\alpha_{21}} = \frac{k_{-21}\beta_{21}k_{22}\alpha_{12}}{k_{21}\beta_{12}k_{-22}\alpha_{21}} = 1 \tag{8}$$

Focusing on the kinetic transitions among 4 different states of the enzyme, Scheme 2 can be simplified to Scheme 3, according to the property of pseudo-first-order kinetics of substrate or product binding. This is equivalent to the conventional ensemble steady-state approximation in which the substrate and product concentrations are treated to be time-independent approximately. The solution of the steady-state probability P^{ss} of Scheme 3 (same as Scheme 2) can be solved by the standard eigenvector approach [Eq. (9)]:

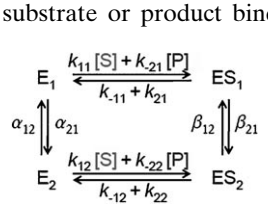

Scheme 3. Kinetic transition of fluctuating enzymes.

$$\begin{aligned}
P^{ss}_{E_1} &= \frac{1}{\Sigma}\big(\beta_{12}(k_{12}[S]+k_{-22}[P])(k_{-11}+k_{21}) + \beta_{12}\alpha_{12}(k_{-11}+k_{21}) \\
&\quad +\alpha_{12}(k_{-11}+k_{21})(k_{-12}+k_{22}) + \alpha_{12}\beta_{21}(k_{-12}+k_{22})\big) \\
P^{ss}_{E_2} &= \frac{1}{\Sigma}\big(\beta_{21}(k_{11}[S]+k_{-21}[P])(k_{-12}+k_{22}) + \beta_{21}\alpha_{21}(k_{-12}+k_{22}) \\
&\quad +\alpha_{21}(k_{-11}+k_{21})(k_{-12}+k_{22}) + \alpha_{21}\beta_{12}(k_{-11}+k_{21})\big) \\
P^{ss}_{ES_1} &= \frac{1}{\Sigma}\begin{pmatrix}\alpha_{12}(k_{11}[S]+k_{-21}[P])(k_{-12}+k_{22}) + \beta_{12}\alpha_{12}(k_{11}[S]+k_{-21}[P]) \\ +\beta_{12}(k_{11}[S]+k_{-21}[P])(k_{12}[S]+k_{-22}[P]) + \alpha_{21}\beta_{12}(k_{12}[S]+k_{-22}[P])\end{pmatrix} \\
P^{ss}_{ES_2} &= \frac{1}{\Sigma}\begin{pmatrix}\alpha_{21}(k_{12}[S]+k_{-22}[P])(k_{-11}+k_{21}) + \beta_{21}\alpha_{21}(k_{12}[S]+k_{-22}[P]) \\ +\beta_{21}(k_{11}[S]+k_{-21}[P])(k_{12}[S]+k_{-22}[P]) + \alpha_{12}\beta_{21}(k_{11}[S]+k_{-21}[P])\end{pmatrix}
\end{aligned} \tag{9}$$

in which Σ is the normalization factor satisfying $P^{ss}_{E_1} + P^{ss}_{E_2} + P^{ss}_{ES_1} + P^{ss}_{ES_2} = 1$.

The net enzyme velocity v_{net} is related to the steady-state probabilities of ES_1, ES_2, E_1, and E_2 through the following relation [Eq. (10)]:

$$\begin{aligned}
v_{net} &= P^{ss}_{ES_1}\cdot k_{21} + P^{ss}_{ES_2}\cdot k_{22} - P^{ss}_{E_1}\cdot k_{-21}[P] - P^{ss}_{E_2}\cdot k_{-22}[P] \\
&= \frac{A[S]^2 + B[S][P] + C[P]^2 + D[S] + E[P]}{F[S]^2 + G[S][P] + H[P]^2 + I[S] + J[P] + K}
\end{aligned} \tag{10}$$

In which [Eq. (11)]:

$$\begin{aligned}
A &= k_{11}k_{12}(\beta_{12}k_{21} + \beta_{21}k_{22}) \\
B &= \beta_{12}k_{21}k_{11}k_{-22} + \beta_{21}k_{22}k_{12}k_{-21} - \beta_{12}k_{-21}k_{-11}k_{12} - \beta_{21}k_{-22}k_{-12}k_{11} \\
C &= -k_{-21}k_{-22}(\beta_{12}k_{-11} + \beta_{21}k_{-12}) \\
D &= \alpha_{12}k_{21}k_{11}k_{-12} + \alpha_{12}k_{21}k_{11}k_{22} + \alpha_{21}k_{22}k_{12}k_{-11} + \alpha_{21}k_{22}k_{12}k_{21} \\
&\quad +\alpha_{12}\beta_{12}k_{21}k_{11} + \alpha_{21}\beta_{12}k_{21}k_{12} + \alpha_{21}\beta_{21}k_{22}k_{12} + \alpha_{12}\beta_{21}k_{22}k_{11} \\
E &= -\begin{pmatrix}\alpha_{12}k_{-21}k_{-11}k_{-12} + \alpha_{12}k_{-21}k_{-11}k_{22} + \alpha_{21}k_{-22}k_{-11}k_{-12} + \alpha_{21}k_{-22}k_{21}k_{-12} + \\ \alpha_{12}\beta_{12}k_{-21}k_{-11} + \alpha_{21}\beta_{12}k_{-22}k_{-11} + \alpha_{21}\beta_{21}k_{-22}k_{-12} + \alpha_{12}\beta_{21}k_{-21}k_{-12}\end{pmatrix} \\
F &= k_{11}k_{12}(\beta_{12} + \beta_{21}) \\
G &= (\beta_{12} + \beta_{21})(k_{11}k_{-22} + k_{12}k_{-21}) \\
H &= k_{-21}k_{-22}(\beta_{12} + \beta_{21}) \\
I &= (\beta_{12} + \alpha_{21})k_{12}(k_{-11} + k_{21}) + (\beta_{21} + \alpha_{12})k_{11}(k_{-12} + k_{22}) + \\
&\quad (\beta_{12} + \beta_{21})(\alpha_{12}k_{11} + \alpha_{21}k_{12}) \\
J &= (\beta_{12} + \alpha_{21})k_{-22}(k_{-11} + k_{21}) + (\beta_{21} + \alpha_{12})k_{-21}(k_{-12} + k_{22}) + \\
&\quad (\beta_{12} + \beta_{21})(\alpha_{12}k_{-21} + \alpha_{21}k_{-22}) \\
K &= (\alpha_{12} + \alpha_{21})[(k_{-12} + k_{22})(k_{-11} + k_{21}) + \beta_{21}(k_{-12} + k_{22}) + \beta_{12}(k_{-11} + k_{21})]
\end{aligned} \tag{11}$$

Note that among above parameters A–K, C and E are always negative, the sign of B depends on the kinetic parameters, and the rest are always positive.

Phase Diagram of the Complex Kinetics of Fluctuating Enzymes

One can see two general features about the kinetics described by Equation (10). First, the dependence on substrate or product concentrations is generally non-Michaelis–Menten. Several recent theoretical studies have worked out a few special conditions (e.g., quasi-static condition, quasi-equilibrium condition, and so forth) under which the hyperbolic MM kinetics still holds for fluctuating enzymes.[28-31] Here in the present paper, however, we will explore the whole "phase space" of the kinetic behavior. Second, the functional dependence of Equation (10) on substrate concentration and product concentration is the same. Such symmetry between substrate and product can be regarded as a generalization of the classic Haldane relation.

Generalized EH Plot for Fluctuating Enzymes

As we have done in Equation (5) for Scheme 1, we now try to build a generalized EH plot for Schemes 2 and 3. Replacing $[S]$ with $\Delta S+([P]/K_{eq})$ as in Equation (3), we can simplify the numerator and re-write the denominator of Equation (10) by repetitively applying the Haldane relation, Equation (7), and detailed balance condition, Equation (8), to get Equations (12) and (13):

$$\begin{aligned} &A[S]^2 + B[S][P] + C[P]^2 + D[S] + E[P] = \\ &A\Delta S^2 + \left[2A([P]/K_{eq}) + B[P] + D\right]\Delta S \end{aligned} \tag{12}$$

$$\begin{aligned} &F[S]^2 + G[S][P] + H[P]^2 + I[S] + J[P] + K \\ &= F\Delta S^2 + \left[2F([P]/K_{eq}) + G[P] + I\right]\Delta S \\ &+\left[F([P]/K_{eq})^2 + G[P]^2/K_{eq} + H[P]^2 + I([P]/K_{eq}) + J[P] + K\right] \end{aligned} \tag{13}$$

As in Equation (5), to construct the generalized EH plot for fluctuating enzyme, we first define the Y and X axes of the generalized EH plot, [Eq. (14)]:

$$\begin{aligned} Y &\equiv v_{net} = \frac{c_1^{[P]}\Delta S^2 + c_2^{[P]}\Delta S}{c_3^{[P]}\Delta S^2 + c_4^{[P]}\Delta S + c_5^{[P]}} \\ X &\equiv \frac{v_{net}}{\Delta S} = \frac{c_1^{[P]}\Delta S + c_2^{[P]}}{c_3^{[P]}\Delta S^2 + c_4^{[P]}\Delta S + c_5^{[P]}} \end{aligned} \tag{14}$$

in which the coefficients $c_i^{[P]}$ are dependent on $[P]$ in general. Comparing with Equation (12), one can have the explicit expressions [Eq. (15)]:

$$\begin{aligned} c_1^{[P]} &= A \\ c_2^{[P]} &= \left(\frac{2A}{K_{eq}} + B\right)[P] + D \\ c_3^{[P]} &= F \\ c_4^{[P]} &= \left(\frac{2F}{K_{eq}} + G\right)[P] + I \\ c_5^{[P]} &= \left(\frac{F}{K_{eq}^2} + \frac{G}{K_{eq}} + H\right)[P]^2 + \left(\frac{I}{K_{eq}} + J\right)[P] + K \end{aligned} \tag{15}$$

Based on the explicit expressions from A to K in Equation (11), we note that all these five $c_i^{[P]}$ are always positive, for all non-negative $[P]$. This property will be used later. The parametric forms of Equation (14) indicates that the Y–X curve satisfy the following bivariate quadratic form in generalized EH plot [Eq. (16)]:

$$c_3^{[P]}Y^2 + c_4^{[P]}XY + c_5^{[P]}X^2 - c_1^{[P]}Y - c_2^{[P]}X = 0 \tag{16}$$

The equation can result in an ellipsoidal, hyperbolic, or parabolic relation, depending on the specific $c_i^{[P]}$ parameters.

Key Parameters $T^{[P]}$ and $R^{[P]}$ for Phase Diagram of Complex Kinetics

Recall that in Equation (5), the negative slope of the generalized EH plot is the apparent Michaelis constant. However, the complication for Equation (14) is that the slope of the generalized EH plot (Y–X curve) is not a constant. So, we first compute the negative slopes of the Y–X curve at small ΔS and large ΔS limits [Eq. (17)]:

$$-\frac{dY}{dX} = -\left(\frac{c_1\Delta S^2 + c_2\Delta S}{c_3\Delta S^2 + c_4\Delta S + c_5}\right)' \Big/ \left(\frac{c_1\Delta S + c_2}{c_3\Delta S^2 + c_4\Delta S + c_5}\right)' \tag{17}$$

The $-dY/dX \rightarrow c_2c_5/(c_2c_4-c_1c_5)$ applies when $\Delta S \rightarrow 0$, and applies $-dY/dX \rightarrow (c_1c_4-c_2c_3)/c_1c_3$ when $\Delta S \rightarrow \infty$.

Based on the sign and the relative amplitudes of the above two apparent Michaelis constants at two limits, we now introduce two key parameters $T^{[P]}$ and $R^{[P]}$ in this paper [Eq. (18)]:

$$T^{[P]} \equiv c_1^{[P]}c_4^{[P]} - c_2^{[P]}c_3^{[P]},\ R^{[P]} \equiv \frac{c_1^{[P]}(c_2^{[P]}c_4^{[P]} - c_1^{[P]}c_5^{[P]})}{\left(c_2^{[P]}\right)^2 c_3^{[P]}} \tag{18}$$

Since all five $c_i^{[P]}$ are always positive, one can verify that 1) $T^{[P]}$ gives the sign of the negative slope of the Y–X curve when $\Delta S \rightarrow \infty$, 2) $R^{[P]}$ gives the sign of the negative slope of the Y–X curve when $\Delta S \rightarrow 0$, and 3) when both $T^{[P]}$ and $R^{[P]}$ are positive, $R^{[P]}=1$ means the above two slopes are identical.

Graphical and Numerical Features of the Phase Diagram

We show in Table 1 and Figure 1 that distinct non-MM phase regions can be classified by the combinations of $T^{[P]}$ and $R^{[P]}$ parameters, as denoted as phase **SI** (substrate inhibition), **SM** (sigmoidal), **CVB** (convex biphasic), and **CCB** (concave biphasic). The classic MM kinetics are restored when $R^{[P]}=1$ and $T^{[P]}>0$.

Table 1. Properties of phase regions of non-MM kinetics.

Phase	Michaelis–Menten MM	Substrate inhibition SI	Sigmoidal SM	Convex biphasic CVB	Concave biphasic CCB
T	$T>0$	$T<0$	$T>0$	$T>0$	$T>0$
R	1	$0<R<1$	$R<0$	$0<R<1$	$R>1$
$\left(\frac{d^2Y}{d(\Delta S)^2}\right)_{\Delta S\to 0}$	<0	<0	>0	<0	<0
Hill coefficient	1	>1[a]	(1, 2)	(1, 2)	(0, 1)
cooperativity	non	positive[a]	positive	positive	negative

[a] We discuss the cooperativity behavior for SI phase only in the condition that the substrate inhibition has not occurred yet in the experimental range of substrate concentration.

Table 2. Kinetic parameters of phase regions of non-MM kinetics.

	Figure 2 Substrate inhibition	Figure 3 Sigmoidal	Figure 4 Convex biphasic	Figure 5 Concave biphasic
k_{11}	959.4425	1.1092e+003	341.6867	6.4836e+003
k_{21}	252.0431	860.1140	34.3467	623.0118
$k_{<M->11}$	1.4833	25.6113	99.3434	1.6197e+004
$k_{<M->21}$	1.6303e+005	3.7252e+004	118.1338	249.3855
k_{12}	324.7520	6.1036	7.1054e+003	20.7018
k_{22}	3.7775e+003	1.9645	1.2928e+003	3.4229e+003
$k_{<M->12}$	1.5572e+003	461.4864	14.6513	2.5389
$k_{<M->22}$	787.8102	0.0260	6.2698e+005	2.7910e+004
α_{12}	1.3679	1.0772	1.9102e+003	1.5685e+003
α_{21}	36.5748	186.3525	307.7835	157.6521
β_{12}	13.8399	307.1485	262.7799	5.0252e+003
β_{21}	0.1193	16.2263	5.9700e+003	1.0288e+004
T	−8.0018	5.0142	0.2468	124.7403
R	0.1531	−148.6055	0.3793	2.5351
$[P]$	0	0	0	0
K_{eq}	1	1	1	1

Before we investigate the implications of the phase regions in enzymology, we first provide typical numerical examples of the above four situations. All the kinetic parameters k_{11}, k_{-11}, k_{21}, k_{-21}, k_{12}, k_{-12}, k_{22}, k_{-22}, α_{12}, α_{21}, β_{12}, β_{21} in Scheme 2 are randomly generated under the constraints of the Haldane relation, Equation (7), and detailed balance, Equation (8). For the sake of simplicity, we choose $[P]=0$ and $K_{eq}=1$. The randomly generated kinetic parameters, as well as the resulting T and R parameters, are tabulated in Table 2. The results are relatively robust. In order for better illustration, we employ three different plots: the conventional Michaelis–Menten plot (Y is plotted as a function of ΔS), the generalized EH plot (Y is plotted as a function of X) and the empirical Hill plot (discussed in the following), as depicted in Figures 2–5.

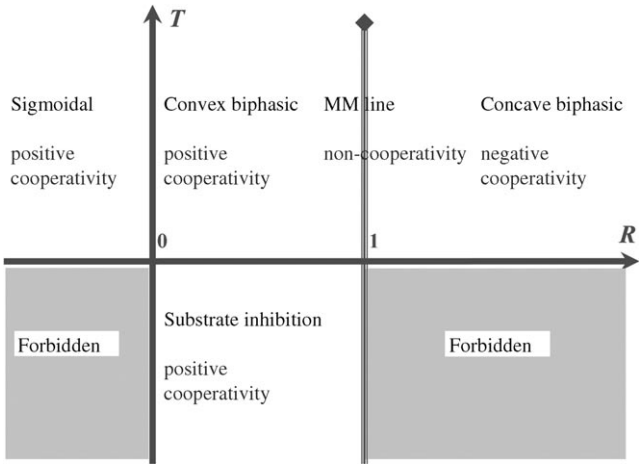

Figure 1. Phase diagram of the kinetics of fluctuating enzymes. Distinct non-MM kinetics of Scheme 2 can be classified by the combinations of $T^{[P]}$ and $R^{[P]}$ defined in Equation (18): phase substrate inhibition (**SI**), sigmoidal (**SM**), convex biphasic (**CVB**) and concave biphasic (**CCB**). The classic MM kinetics holds when $R^{[P]}=1$ and $T^{[P]}>0$. Two forbidden regions are illustrated: 1) the region of $T^{[P]}<0$ and $R^{[P]}>1$; 2) the region of $T^{[P]}<0$ and $R^{[P]}<0$. Functionally, **SI**, **SM**, and **CVB** exhibit positive cooperativity, whereas **CCB** displays negative cooperativity. Obviously, MM kinetics corresponds to non-cooperativity.

For the empirical Hill plot, $Y/(\max(Y)-Y)$, in which $\max(Y)$ is the maximum value of net velocity Y, is plotted as a function of ΔS in the log–log manner.[32-39] In the case of classic MM kinetics shown in Equations (4) and (5), $Y=k_2\Delta S\Big/\left(K_M^{[P]}+\Delta S\right)$, thus, the slope of the curve, which is defined as the Hill coefficient, is unity. As a consequence, the non-unity Hill coefficient is widely used as an index of cooperativity, the degree of cooperativity being considered to increase as the coefficient increases: a Hill coefficient being greater than unity means positive cooperativity, whereas being smaller than unity means negative cooperativity.

Enzymological Meanings of the Phase Diagram of the Kinetics

In this section we will rigorously demonstrate the enzymological meanings of the various complex kinetic phases, and the connection to corresponding regimes in the phase diagram.

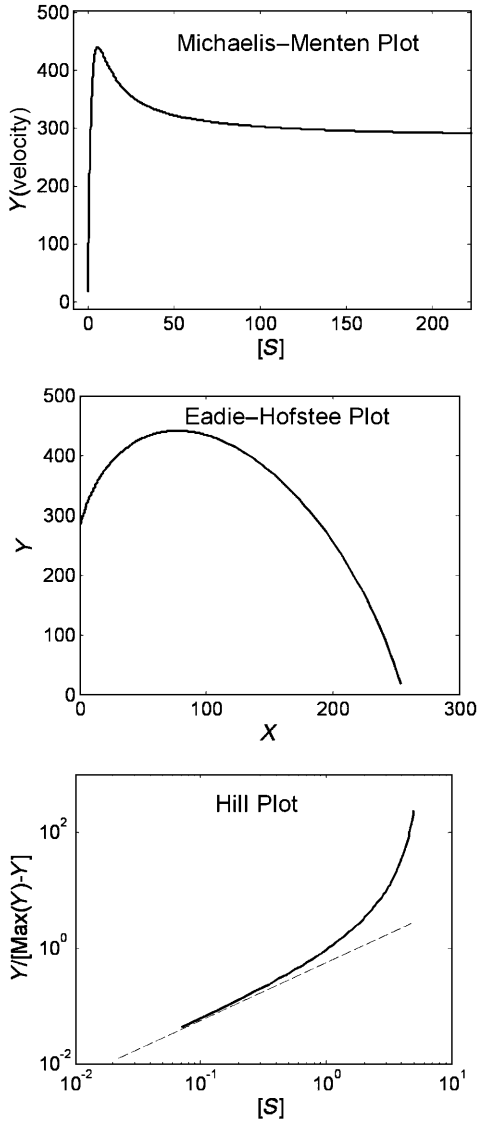

Figure 2. Plots showing substrate inhibition.

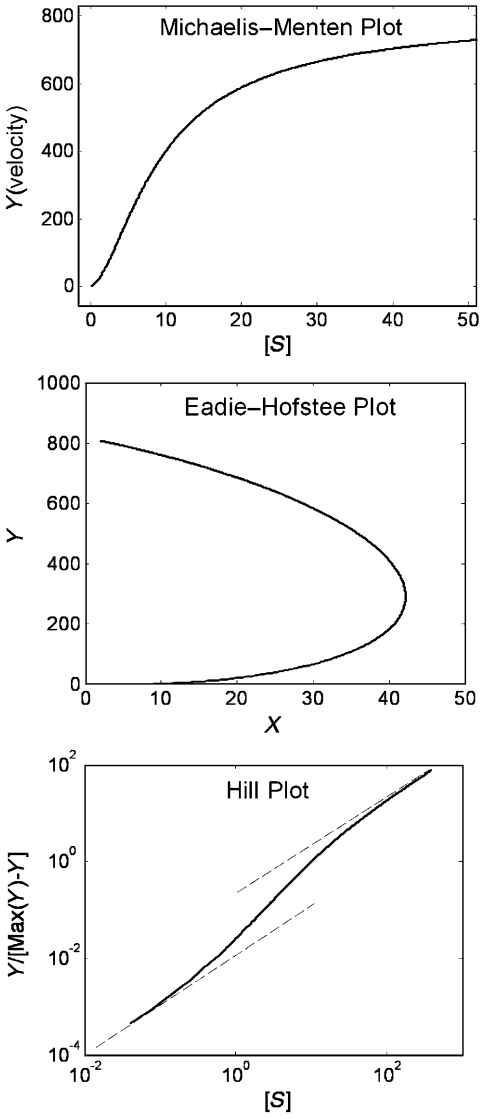

Figure 3. Plots showing a sigmoidal relationship.

Phase Substrate Inhibition (SI)

Let us first prove that **Phase SI** ($T^{[P]}<0$) corresponds to excess substrate inhibition. Based on Equation (14), we can calculate Equations (19):

$$\frac{dY}{d(\Delta S)}=\frac{(c_1c_4-c_2c_3)\Delta S^2+2c_1c_5\Delta S+c_2c_5}{(c_3\Delta S^2+c_4\Delta S+c_5)^2} \qquad (19)$$

Since all five $c_i^{[P]}$ are always positive, it is clear from Equation (19) that when and only when $T=c_1c_4-c_2c_3<0$, $dY/d(\Delta S)$ can be zero or negative for a certain range of ΔS. Such a negative value of $dY/d(\Delta S)$ certainly reflects the phenomenon of excess substrate inhibition.

We note that the above mechanism for substrate inhibition is very different from the one discussed in most textbooks and in the literature. In the textbook kinetic scheme,[6] when substrate concentration is sufficiently high, two (or more) substrate molecules are assumed to bind to the enzyme active site in the same place at the same time, interfere with each other, and de-activate the whole *ESS* complex. However, in Scheme 2, there is at most one substrate molecule bound within the active site at any given instant. Therefore, it will be worthwhile noting this new mechanism of substrate inhibition and discriminating it from the conventional textbook model.

Positive Cooperativity (Phase SM and CVB) and Negative Cooperativity (Phase CCB)

We now prove that **Phase SM** and **CVB** correspond to positive cooperativity, and **Phase CCB** corresponds to negative cooperativity, by computing the well-adopted Hill coefficient. Note that **Phase SM**, **CVB**, and **CCB** are all under $T^{[P]}>0$, thus, no substrate inhibition exists, and $Max(Y)=c_1/c_3$ is the asymptote value when $\Delta S\rightarrow\infty$. Sub-

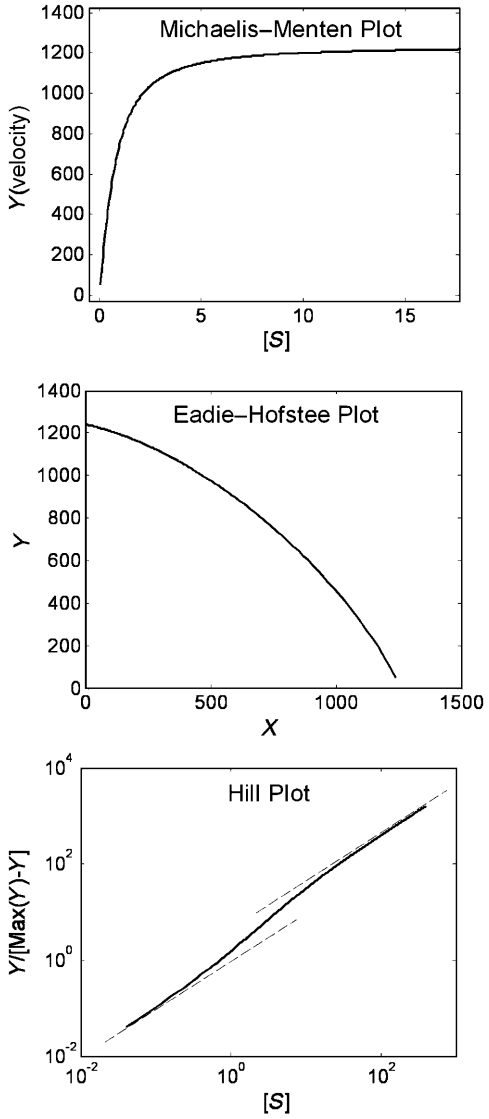

Figure 4. Plots showing a convex biphasic relationship.

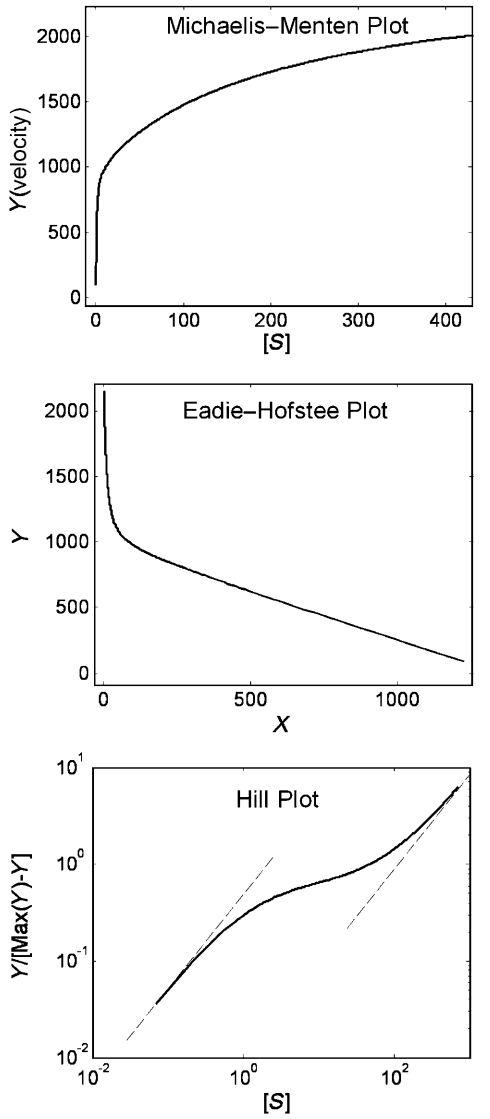

Figure 5. Plots showing a concave biphasic relationship.

stituting Equation (14) into $Y/(\max(Y)-Y)$ of the Hill plot, we have Equation (20)

$$\log(Y/(\max(Y)-Y)) = \log\Delta S + \log\frac{\Delta S+(c_2/c_1)}{\Delta S+[c_1c_5/(c_1c_4-c_2c_3)]} + \log\frac{c_1c_3}{c_1c_4-c_2c_3} \quad (20)$$

For **Phase SM** and **CVB**, $R^{[P]}<1$ and $T^{[P]}>0$, which is equivalent to $0<c_2/c_1<c_1c_5/(c_1c_4-c_2c_3)$. For **Phase CCB**, $R^{[P]}>1$ and $T^{[P]}>0$, which is equivalent to $c_2/c_1>c_1c_5/(c_1c_4-c_2c_3)>0$.

The second term in the right side of Equation (20) increases with ΔS increasing when $0<c_2/c_1<c_1c_5/(c_1c_4-c_2c_3)$, whereas it decreases with ΔS increasing when $c_2/c_1>c_1c_5/(c_1c_4-c_2c_3)>0$. Moreover, for the former case, it can be shown that the Hill coefficient (the slope of $\log(Y/(\max(Y)-Y))$ vs $\log\Delta S$) is bound within (1, 2), which by convention corresponds to the positive cooperativity. The upper bound of 2 for Hill coefficient arises from the highest order dependence on substrate and product concentrations being quadratic in this minimal model. For the latter case, the Hill coefficient is bound within (0, 1), which corresponds to the negative cooperativity. Therefore, the $R^{[P]}$ parameter is indeed an indicator for positive/non/negative cooperativity.

Positive Cooperativity and Sigmoidal (Phase SM and CVB)

Although it is clear that **Phase SM** and **CVB** both correspond to positive cooperativity (owing to $R^{[P]}<1$), they still have different R parameters: $R^{[P]}<0$ in **Phase SM**, and $R^{[P]}>0$ in **Phase CVB**. The distinction can be illustrated by computing the second derivative of the Y versus ΔS function when $\Delta S\rightarrow 0$, [Eq. (21)]:

$$\left(\frac{d^2Y}{d(\Delta S)^2}\right)_{\Delta S\to 0}=\frac{2(c_1c_5-c_2c_4)}{c_5^2} \tag{21}$$

Clearly, $R^{[P]}<0$ in **Phase SM** indicates a positive second derivative, meaning that in the conventional Michaelis–Menten plot the curve is concave up at small ΔS. Such a graphical feature, exhibited by the numerical example in Figure 3, is typical of the "sigmoidal"(S-shaped) kinetics.

The difference between **Phase SM** and **CVB** also highlights an interesting point which has not been well appreciated in the enzymology literature. Not all the positive cooperativity kinetics are sigmoidal. For example, **Phase CVB** exhibits positive cooperativity but it is not sigmoidal in shape. These two terms are defined for different purposes. In other words, sigmoidal kinetics are a sufficient but not necessary condition for positive cooperativity.

Positive Cooperativity for Substrate Inhibition (Phase SI)

Now we discuss the cooperativity behavior associated with substrate inhibition (**Phase SI**), although these two topics are usually not analyzed together in the current literature. This is indeed a subtle point. On one hand, such non-correlation between substrate inhibition and cooperativity is justifiable because $\log(Y/(\max(Y)-Y))$ in the Hill plot is unbounded if substrate inhibition occurs (because of the vanishing denominator in the course). On the other hand, practically, the first half portion of the Hill plot can be approximately constructed if substrate inhibition has not occurred yet in the experimental range of substrate concentration, with $\max(Y)$ chosen to be the asymptote enzyme velocity before the inhibition takes over. In this practical scenario, the Hill coefficient would be greater than one. This is because $R^{[P]}<1$ if $T^{[P]}<0$, and $R^{[P]}<1$ means positive cooperativity. This phenomenon is illustrated in Figure 2.

Forbidden Regions in the Phase Diagram

Besides the permissible phases discussed above, there are two distinct forbidden regions in the phase diagram (Figure 1): 1) the region of $T^{[P]}<0$ and $R^{[P]}>1$ implies that negative cooperativity and substrate inhibition cannot coexist; 2) the region of $T^{[P]}<0$ and $R^{[P]}<0$ implies that sigmoidal and substrate inhibition contradict with each other in our minimal model.

The first forbidden region of $T^{[P]}<0$ and $R^{[P]}>1$ can be easily demonstrated by the fact that $R^{[P]}<1$ if $T^{[P]}<0$, based on Equation (18). However, the conjecture of the second forbidden region of $T^{[P]}<0$ and $R^{[P]}<0$ is more difficult to prove, since it involves detailed functional dependence of $c_i^{[P]}$ on parameters A through K in Equation (11). Fortunately, one can easily test the claims about these two forbidden regions numerically. Millions of groups of k_{11}, k_{-11}, k_{21}, k_{-21}, k_{12}, k_{-12}, k_{22}, k_{-22}, α_{12}, α_{21}, β_{12}, β_{21} (consistent with the constraint of the Haldane relation and detailed balance) are generated randomly, the corresponding $T^{[P]}$ and $R^{[P]}$ parameters are calculated, and none of them shows up in the forbidden regions.

The above cooperativity phenomenon (except substrate inhibition) for enzymes with a single binding site has been loosely termed as "kinetic cooperativity" according to a number of researchers,[32–38] to discriminate it from the classic MWC (concerted) and KNF (sequential) models for the equilibrium binding curves of multi-subunit enzymes.[2–6,39] But these earlier studies [32–38] were somewhat less comprehensive and quantitative. Especially, the different behaviors of non-MM kinetics were not treated in a unified framework.

Product Induced Phase Transition of the Enzyme Kinetics

In this section, we elaborate on an interesting but unexplored phenomenon: non-MM behaviors could undergo transitions among different kinetic phases induced by varying product concentrations.

Such a transition may be regarded as the manifestation of modification of the steady-state probabilities of ES_1, ES_2, E_1, and E_2 owing to changes of product concentration in a nonlinear manner. To the contrast, recall that in the classic MM scheme, the only effect of $[P]$ is to modify the apparent $K_M^{[P]}$ linearly through Equation (5).

Plugging the explicit $[P]$ dependence of $c_i^{[P]}$ into the $T^{[P]}$ parameter in Equation (18), then we have Equation (22):

$$T^{[P]}=(AG-BF)[P]+(AI-DF) \tag{22}$$

From Equation (11), it is easy to prove that $AG-BF$ is always positive. Therefore, $T^{[P]}$ is a monotonic increasing function of $[P]$. Such a linear dependence of $T^{[P]}$ on $[P]$ has an interesting effect on substrate inhibition. With $[P]$being sufficiently high and greater than a critical value $[P]_C$, [Eq. (23)]:

$$[P]_C=\frac{DF-AI}{AG-BF} \tag{23}$$

$T^{[P]}$ would change its sign from negative to positive, suggesting that this enzyme-substrate-product system exhibit a transition escaping from **Phase SI**. Apparently, $[P]_C$ is negative if $AI-DF>0$, showing that there is no substrate inhibition at any non-negative $[P]$. This is equivalent to $T^{[P]}>0$.

The explicit $[P]$ dependence of the $R^{[P]}$ parameter is more complicated than that of the $T^{[P]}$ parameter, as shown in the following Equation (24)

$$R^{[P]}=\frac{A}{F}\frac{\left(\frac{3AF}{K_{eq}^2}+\frac{AG+2BF}{K_{eq}}+BG-AH\right)[P]^2+\left(\frac{2DF+AI}{K_{eq}}+DG+BI-AJ\right)[P]+(DI-AK)}{\left(\frac{2A}{K_{eq}}+B\right)^2[P]^2+2D\left(\frac{2A}{K_{eq}}+B\right)[P]+D^2} \tag{24}$$

This tells us that the cooperativity behavior of the enzyme, i.e., whether it is positive, negative, or non-coopera-

tive, is changing with the varying product concentration in a very complicated way.

To illustrate the phenomenon of product induced phase evolution and phase transition, we now take the kinetic parameters of substrate inhibition in Figure 2 as an example. In the case of Figure 2, $[P]=0$, and the associated $T=-8.0018$, $R=0.1531$. As shown in Figure 6a, when $[P]$is increasing from zero, $T^{[P]}$ and $R^{[P]}$ evolve obeying

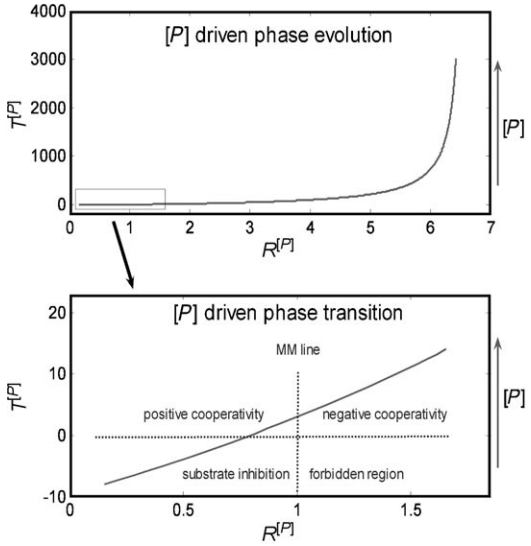

Figure 6. Product induced kinetic phase evolution and phase transition. The phase starts from **SI** in which $[P]=0$, $T=-8.0018$, $R=0.1531$.

Equations (22) and (24), respectively. Figure 6b depicts a finer path of the phase evolution and transitions of Figure 6a. The phase point starts from substrate inhibition, crosses the boundary of $T^{[P]}=0$ and becomes positive cooperativity (convex biphasic), and then passes through the Michaelis–Menten line and ends up with negative cooperativity (concave biphasic).

Such a phenomenon of product concentration dependent kinetics could have implications to enzyme functions in living cells, considering the fact that most knowledge on enzyme kinetics is obtained in vitro in the absence of products, whereas the actual enzymes always perform functions in the presence of products in vivo.

Conclusions

As systematically analyzed in this study, the fluctuating enzyme with only two conformational channels can display surprisingly complex and versatile kinetic behaviors (phases) including substrate inhibition (**SI**), sigmoidal kinetics (**SM**), convex biphasic (**CVB**), and concave biphasic (**CCB**). By calculating the corresponding Hill coefficients, we prove that the first three phases exhibit positive cooperativity, whereas the last one shows negative cooperativity. The lesson from such a minimal model is that, all these seemingly unrelated kinetic phases are actually interrelated and can be adequately described by a unified two-dimensional phase diagram parameterized by $T^{[P]}$ and $R^{[P]}$. These complex kinetics are produced by fluctuating enzymes with a single binding site, which is fundamentally different from the classic MWC and KNF models for equilibrium binding of multi subunit enzymes.

Refs. [50–64] list ten recent experimental enzyme systems which have been measured to display distinct non-MM kinetics including **SI**, **SM**, **CVB**, and **CCB**. Since the enzymes are all *monomeric* in function, the classic MWC and KNF models are not applicable. Therefore, the fluctuating enzyme notion might be responsible for some of the observed non-MM kinetics.

In the perspective of dynamic disorder and dispersed kinetics for enzyme catalysis, one often adopts multiple concrete states or a continuum model for conformational diffusion.[28–31] However, such a general treatment either includes too many parameters of rate constants (for the multiple concrete states)[28] or contains unknown functional form of the coordinate dependent rate constants (in the continuum model for conformational diffusion),[29–31] which makes the thorough evaluation of the complex kinetics difficult. Recently, models based on two-dimensional reaction free energy surface [40–41] and non-equilibrium steady states [42–46] have been developed to account for kinetic cooperativity, but again involve many parameters and detailed knowledge on free energy surfaces. We also note that several theoretical studies have been recently performed along the line of Kramers' escape model with power-law friction kernel instead of the conventional fast-decaying friction kernel.[47–49] As minimal as it can be, Scheme 2 allows one to unite and understand the whole phase–space kinetic behaviors with reasonable computational complexity. Such a two channel scheme represents the lowest-order generalization of the classic MM scheme, by only including the quadratic dependence of substrate and product concentrations.

As a prediction of this paper, these non-MM behaviors depend intrinsically on the product concentration owing to the underlying Haldane symmetry between the substrate and product, and could undergo transitions among different kinetic phases induced by varying product concentrations. We believe such an effect of product has implications to the understanding of enzyme kinetics in living cells. On one hand, almost all the kinetic parameters and properties of enzymes are characterized in vitro through the initial rate measurement (e.g., stopped flow) in which the product concentration is negligible. On the other hand, the product molecules are certainly non-zero in the cellular environment in vivo. Therefore, according to our observation, the actual kinetic phases that enzymes occupy in vivo might be different from what they are measured in vitro in the absence of product. This can be tested by performing the net rate measurement in the presence of both substrate and product premixed with an appropriate ratio.

Acknowledgements

We are grateful to S. C. Kou, Brian English, Binny Cherayil, Hong Qian, and Jianhua Xing for helpful discussions. X.S.X. acknowledges DOE (Office of Basic Energy Science) for support.

[1] R. Wolfenden, M. J. Snider, *Acc. Chem. Res.* **2001**, *34*, 938–945.
[2] D. L. Nelson, M. M. Cox, *Lehninger Principles of Biochemistry 4th ed.,* W. H. Freeman and Company, New York, **2004**.
[3] G. G. Hammes, *Enzyme Catalysis and Regulation*, Academic Press, New York, **1982**.
[4] A. Fersht, *Enzyme Structure and Mechanism*, *2nd ed.*, W. H. Freeman, New York, **1985**.
[5] I. H. Segel, *Enzyme Kinetics: Behavior and Analysis of Rapid Equilibrium and Steady-State Enzyme Systems*, Wiley, New York, **1993**.
[6] A. Cornish-Bowden, *Fundamentals of enzyme kinetics*, *2nd ed.*, Portland Press, **1995**.
[7] L. Michaelis, M. L. Menten, *Biochem. Z.* **1913**, *49*, 333–362.
[8] G. E. Briggs, J. B. S. Haldane, *Biochem. J.* **1925**, *19*, 338–339.
[9] J. B. S. Haldane, *Enzymes*, Longmans, London, **1930**.
[10] C. L. Brooks, III., M. Karplus, B. M. Pettitt, *Advances in Chemical Physics, Proteins: A Theoretical Perspective of Dynamics, Structure, & Thermodynamics, Vol. 71*, Wiley-Interscience, **1988**.
[11] H. Frauenfelder, S. G. Sligar, P. G. Wolynes, *Science* **1991**, *254*, 1598.
[12] H. Yang, G. Luo, P. Karnchanaphanurach, T.-M. Louie, I. Rech, S. Cova, L. Xun, X. S. Xie, *Science* **2003**, *302*, 262.
[13] S. C. Kou, X. S. Xie, *Phys. Rev. Lett.* **2004**, *93*, 180603.
[14] W. Min, G. Luo, B. J. Cherayil, S. C. Kou, X. S. Xie, *Phys. Rev. Lett.* **2005**, *94*, 198302.
[15] E. Z. Eisenmesser, O. Millet, W. Labeikovsky, D. M. Korzhnev, M. Wolf-Watz, D. A. Bosco, J. J. Skalicky, L. E. Kay, D. Kern, *Nature* **2005**, *438*, 117–121.
[16] H. P. Lu, L. Xun, X. S. Xie, *Science* **1998**, *282*, 1877.
[17] R. J. Davenport, G. J. Wuite, R. Landick, C. Bustamante, *Science* **2000**, *287*, 2497–2500.
[18] G. J. Wuite, S. B. Smith, M. Young, D. Keller, C. Bustamante, *Nature* **2000**, *404*, 103–106.
[19] X. Zhuang, H. Kim, M. J. B. Pereira, H. P. Babcock, N. G. Walter, S. Chu, *Science* **2002**, *296*, 1473.
[20] A. M. van Oijen, P. C. Blainey, D. J. Crampton, C. C. Richardson, T. Ellenberger, X. S. Xie, *Science* **2003**, *301*, 1235.
[21] O. Flomenbom, K. Velonia, D. Loos, S. Masuo, M. Cotlet, Y. Engelborghs, J. Hofkens, A. E. Rowan, R. J. M. Nolte, M. van der Auweraer, F. C. de Schryver, J. Klafter, *Proc. Natl. Acad. Sci. USA* **2005**, *102*, 2368.
[22] W. Min, B. P. English, G. Luo, B. J. Cherayil, S. C. Kou, X. S. Xie, *Acc. Chem. Res.* **2005**, *38*, 923–931.
[23] B. P. English, W. Min, A. M. van Oijen, K. T. Lee, G. Luo, H. Sun, B. J. Cherayil, S. C. Kou, X. S. Xie, *Nat. Chem. Biol.* **2006**, *2*, 87.
[24] N. S. Hatzakis, H. Engelkamp, K. Velonia, J. Hofkens, P. C. M. Christianen, A. Svendsen, S. A. Patkar, J. Vind, J. C. Maan, A. E. Rowan, R. J. M. Nolte, *Chem. Commun.* **2006**, 2012–2014.
[25] D. E. Koshland, Jr., *Proc. Natl. Acad. Sci. USA* **1958**, *44*, 98–104.
[26] S. Yang, J. Cao, *J. Chem. Phys.* **2002**, *117*, 10996.
[27] H. Qian, *J. Phys. Chem. B* **2006**, *110*, 15063–15074.
[28] S. C. Kou, B. J. Cherayil, W. Min, B. P. English, X. S. Xie, *J. Phys. Chem. B* **2005**, *109*, 19068–19081.
[29] I. V. Gopich, A. Szabo, *J. Chem. Phys.* **2006**, *124*, 154712.
[30] X. Xue, F. Liu, Z. Ou-Yang, *Phys. Rev. E* **2006**, *74*, 030902.
[31] W. Min, I. V. Gopich, B. P. English, S. C. Kou, X. S. Xie, A. Szabo, *J. Phys. Chem. B* **2006**, *110*, 20093–20097.
[32] C. Frieden, *J. Biol. Chem.* **1970**, *245*, 5788–5799.
[33] G. R. Ainslie, J. P. Shill, K. E. Neet, *J. Biol. Chem.* **1972**, *247*, 7088–7096.
[34] C. Frieden, *Annu. Rev. Biochem.* **1979**, *48*, 471–489.
[35] K. E. Neet, G. R. Ainslie, *Methods Enzymol.* **1980**, *64*, 192.
[36] A. Cornish-Bowden, A. L. Cardenas, *J. Theor. Biol.* **1987**, *124*, 1–23.
[37] J. Ricard, A. Cornish-Bowden, *Eur. J. Biochem.* **1987**, *166*, 255–272.
[38] K. E. Neet, *Methods Enzymol.* **1995**, *249*, 519–567.
[39] D. E. Koshland, Jr., K. Hamaani, *J. Biol. Chem.* **2002**, *277*, 46841–46844.
[40] W. Min, X. S. Xie, B. Bagchi, *J. Phys. Chem. B* **2008**, *112*, 454–466.
[41] W. Min, X. S. Xie, B. Bagchi, *J. Chem. Phys.* **2009**, *131*, 065104.
[42] S. R. De Groot, P. Mazur, *Non-Equilibrium Thermodynamics*, Dover Publications, Inc., New York, **1984**.
[43] C. Bustamante, J. Liphardt, F. Ritort, *Phys. Today* **2005**, *58*, 43–48.
[44] W. Min, L. Jiang, J. Yu, S. C. Kou, H. Qian, X. S. Xie, *Nano Lett.* **2005**, *5*, 2373–2378.
[45] H. Qian, X. S. Xie, *Phys. Rev. E* **2006**, *74*, 010902.
[46] D. A. Beard, H. Qian, *Biophys. Chem.* **2005**, *114*, 213–220.
[47] W. Min, X. S. Xie, *Phys. Rev. E* **2006**, *73*, 010902.
[48] S. Chaudhury, B. J. Cherayil, *J. Chem. Phys.* **2006**, *125*, 024904.
[49] S. Chaudhury, B. J. Cherayil, *J. Chem. Phys.* **2006**, *125*, 114106.
[50] J. B. Houston, A. Galetin, *Arch. Biochem. Biophys.* **2005**, *433*, 351–360.
[51] W. M. Atkins, *Annu. Rev. Pharmacology Toxicology* **2005**, *45*, 291–310.
[52] E. E. Scott, Y. A. He, M. R. Wester, M. A. White, C. C. Chin, J. R. Halpert, E. F. Johnson, C. D. Stout, *Proc. Natl. Acad. Sci. USA* **2003**, *100*, 13196–13201.
[53] A. P. Koley, J. T. M. Buters, R. C. Robinson, A. Markowitz, F. K. Friedman, *J. Biol. Chem.* **1995**, *270*, 5014–5018
[54] K. E. Neet, R. P. Keenan, P. S. Tippett, *Biochemistry* **1990**, *29*, 770–777.
[55] K. Kamata, M. Mitsuya, T. Nishimura, J. Eiki, Y. Nagata, *Structure* **2004**, *12*, 429–438.
[56] A. M. Simm, C. S. Higgins, S. T. Pullan, M. B. Avison, P. Nuimsup, O. Erdozain, P. M. Bennett, T. R. Walsh, *FEBS Lett.* **2001**, *509*, 350–354.
[57] A. S. Hussein, M. R. Chacon, A. M. Smith, R. Tosado-Acevedo, M. E. Selkirk, *J. Biol. Chem.* **1999**, *274*, 9312–9319.
[58] A. S. Hussein, A. M. Smith, M. R. Chacon, M. E. Selkirk, *Eur. J. Biochem.* **2000**, *267*, 2276–2282.
[59] G. B. Birrell, T. O. Zaikova, A. V. Rukavishnikov, J. F. Keana, O. H. Griffith, *Biophys. J.* **2003**, *84*, 3264–3275.
[60] N. S. Quinsey, A Q. Luong, P. W. Dickson, *J. Neurochem.* **1998**, *71*, 2132–2138.
[61] J. Nakamura, L. Lou, *J. Biol. Chem.* **1995**, *270*, 7347–7353.
[62] V. J. LiCata, N. M. Allewell, *Biophys. Chem.* **1997**, *64*, 225–234.
[63] X. Zhou, S. Kay, M. D. Toney, *Biochemistry* **1998**, *37*, 5761–5769.
[64] F. Vincent, G. J. Davies, J. A. Brannigan, *J. Biol. Chem.* **2005**, *280*, 19649–19655.

Received: November 9, 2009
Published online: March 16, 2010

